

See discussions, stats, and author profiles for this publication at: <https://www.researchgate.net/publication/231205920>

A Damping System for Syringe Pumps Used for Microdialysis with On-Line Electrochemical Detection

ARTICLE *in* ANALYTICAL CHEMISTRY · JULY 1996

Impact Factor: 5.64 · DOI: 10.1021/ac9601977

CITATIONS

16

READS

21

5 AUTHORS, INCLUDING:



Mila Pravda

University College Cork

56 PUBLICATIONS 1,517 CITATIONS

SEE PROFILE



Sophie Sarre

Vrije Universiteit Brussel

127 PUBLICATIONS 3,265 CITATIONS

SEE PROFILE



Yvette Michotte

Vrije Universiteit Brussel

284 PUBLICATIONS 7,200 CITATIONS

SEE PROFILE

A Damping System for Syringe Pumps Used for Microdialysis with On-Line Electrochemical Detection

Miloslav Pravda,[†] Craig A. Marvin,[‡] Sophie Sarre, Yvette Michotte, and Jean-Michel Kauffmann^{*,§}

Department of Pharmaceutical Chemistry and Drug Analysis, Pharmaceutical Institute, Vrije Universiteit Brussel, Laarbeeklaan 103, 1090 Bruxelles, Belgium

A syringe pump damping system for microdialysis, coupled on-line with amperometric detection, was developed. The damping system consisted of an air bubble and a fused silica capillary. A bubble volume of 20 μL and a 15 cm capillary, 50 μm i.d., were found to be optimal for flow rates between 1 and 5 $\mu\text{L min}^{-1}$. Enhancements of detection limit by 2 orders of magnitude were obtained with this experimental setup.

It is well-known that the background noise of electrochemical detectors positioned in flow streams, such as in HPLC and flow injection analysis (FIA), consists of several factors.^{1–3} A significant contribution to the noise is the unstability of the flow rate itself. The flow systems mentioned above produce pulses that affect the flow rate. To lower the short-term flow fluctuations, pulse dampers are generally used.

With a syringe pump, the stepper motor also produces undamped pulses. The latter are small and not significant in the study of millimolar concentrations of biological substances. When micro- and nanomolar concentrations must be detected, the pulses of the pump constitute serious limitations. In electrochemical detection (EC), the steady state current is determined by the hydrodynamic pattern (i.e., flow cell geometry, flow rate, viscosity, etc.), the electrochemical nature of the depolarizer, the electrode material used, etc.^{2,3} For a diffusion-controlled process at a solid electrode, fluctuation in the flow rate will create higher perturbations on the steady state faradaic current than on the background current, which is of pseudocapacitive origin.

Basically, a damper should consist of elastic and resistive elements. In the case of HPLC, the elastic element is usually a flattened coil of stainless steel, and the resistive element is the analytical column. In this work, the proposed damper consists of an air bubble, the elastic element, and a fused silica capillary, the resistive element.

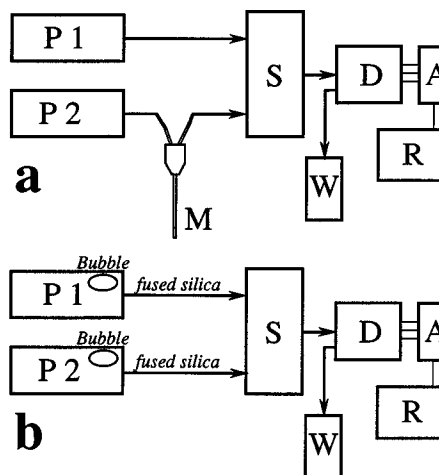


Figure 1. (a) Typical setup of microdialysis coupled on-line with electrochemical detection: P1, P2, syringe pumps (P1, standard solution, P2, blank solution); M, microdialysis probe; S, syringe selector; D, detector; A, amplifier/potentiostat; W, waste; R, recorder (data handling device). (b) Modification used in the present study.

A typical setup for in vivo microdialysis coupled on-line with amperometric detection consists of a peristaltic or syringe pump, a microdialysis probe, and an electrochemical detector (Figure 1). Microdialysis allows the sampling of biological fluids from living tissues without much tissue damage.^{4–7} The microdialysis membrane excludes large molecules (mainly proteins), but electrochemically interfering species such as ascorbate, xanthines, drugs, etc. can still permeate the membrane. Improved selectivity for on-line detection systems can be achieved by incorporating enzymatic biosensors. Such biosensors were successfully applied on-line with microdialysis for subcutaneous glucose (of ~ 10 mM) monitoring in humans by Pfeiffer et al.^{8–12} Similar on-line setups

[†] Permanent address: Department of Analytical Chemistry, Faculty of Chemical Technology, University of Pardubice, Nám. Čs. Legii 565, 532 10 Pardubice, Czech Republic

[‡] Permanent address: BAS EUROPE, Van Maerlantstraat 56, B-2060 Antwerpen, Belgium.

[§] Permanent address: Pharmaceutical Institute, Université Libre de Bruxelles, Campus Plaine, CP 205/6, Boulevard du Triomphe, 1050 Bruxelles, Belgium.

(1) Kissinger, P. T.; Heineman, W. R. *Laboratory Techniques in Electroanalytical Chemistry*; Marcel Dekker: New York, 1984; pp 611–634.

(2) Scott, R. P. W. *Liquid Chromatography Detectors*; Elsevier: Amsterdam, 1986; pp 7–48, 117–123.

(3) Kok, W. T. In *Selective Sample Handling and Detection in High-Performance Liquid Chromatography*; Frei, R. W., Zech, K., Eds.; Elsevier Co.: Amsterdam, 1988; pp 309–363.

(4) Ungerstedt, U. *Measurement of Neurotransmitter Release in vivo*; John Wiley and Sons: New York, 1984; pp 81–105.

(5) Lönnroth, P.; Jansson, P. A.; Smith, U. *Am. J. Physiol.* **1987**, *253*, E228–E231.

(6) Lindefors, N.; Amberg, G.; Ungerstedt, U. *J. Pharmacol. Methods* **1989**, *22*, 141–156.

(7) Sarre, S. Ph.D. Thesis, Vrije Universiteit Brussel, Belgium, 1995; pp 5–48.

(8) Keck, F. S.; Kerner, W.; Meyerhoff, C.; Zier, H.; Pfeiffer, E. F. *Horm. Metab. Res.* **1991**, *23*, 617–618.

(9) Keck, F. S.; Meyerhoff, C.; Kerner, W.; Siegmund, T.; Zier, H.; Pfeiffer, E. F. *Horm. Metab. Res.* **1992**, *24*, 492–493.

(10) Pfeiffer, E. F.; Meyerhoff, C.; Bischof, F.; Keck, F. S.; Kerner, W. *Horm. Metab. Res.* **1993**, *25*, 121–124.

(11) Pfeiffer, E. F. *Horm. Metab. Res.* **1994**, *26*, 510–514.

(12) Meyerhoff, C.; Mennel, F. J.; Bischof, F.; Sternberg, F.; Pfeiffer, E. F. *Horm. Metab. Res.* **1994**, *26*, 538–543.

were also employed in animal pharmacological studies.^{13,14} Other systems were designed for brain glutamate (of $\sim 10 \mu\text{M}$)^{15,16} and subcutaneous lactate (of $\sim 1 \text{ mM}$).¹⁷

In the present study, we present an on-line microdialysis setup with a pulse damper suitable for syringe pumps for the determination of low concentrations of quinones (of $\sim 1 \mu\text{M}$) in brain dialysates in an animal model of stroke.^{18,19} A glassy carbon working electrode was selected since it is more sensitive to aromatic species (quinones) than toward nonaromatic ones (H_2O_2). Hydrogen peroxide (of $\sim 1 \mu\text{M}$) present in the reperfused ischemic brain tissue during the oxidative stress could interfere with electrochemical detection of quinones. Therefore, a low applied potential minimizes the risk of interferences, allowing the selective detection of liberated quinones. In addition, catecholamines present in excess^{20,21} in a ischemic tissue are not detectable at this negative potential.

EXPERIMENTAL SECTION

Reagents. 1,4-Benzoquinone was obtained from Sigma Chemicals (St. Louis, MO) and was dissolved daily as 1 mM stock solution in the perfusion fluid. The perfusion fluid consisted of 147 mM NaCl, 4 mM KCl, and 1 mM HCl, pH 3. This low pH value facilitates the electroreduction of quinones and was used in the studies of the damping effect only. It was not applied for in vivo measurements. All reagents were of analytical grade (Merck, Darmstadt, Germany). The perfusion solution was filtered (BAS filter, pore size $0.2 \mu\text{m}$) before use. Water was purified by a Seralpur Pro 90 CN (Belgolabo, Brussels, Belgium) system (output conductivity $\sim 50 \text{ nS/cm}$).

Apparatus. Two pumps, both with 1 mL Gastight syringes (Hamilton, Reno, NV), were used to control the flow rate: a CMA/100 microinjection pump (CMA Microdialysis AB, Stockholm, Sweden) and a BAS Bee syringe pump (Bioanalytical Systems, W. Lafayette, IN). The UniSwitch syringe selector (Bioanalytical Systems) was used to connect syringes to the on-line detector. The electrochemical detector consisted of a radial thin-layer flow-cell, UniJet²² (BAS), with a glassy carbon working electrode (3 mm i.d., BAS) and a $16 \mu\text{m}$ gasket (BAS) coupled to an LC-4C detector. The detector was connected to a $y-t$ recorder (BAS). Teflon tubing ($120 \mu\text{m}$ i.d., BAS) with a special pressure-resistant connector was used for liquid connections. The 15 cm R-capillary was made from fused silica tubing ($50 \mu\text{m}$ i.d., Achrom, Machelen, Belgium). A Gilson 307 HPLC piston pump (Gilson Medical Electronics, Middleton, WI) was used to estimate the resistance of the R-capillary.

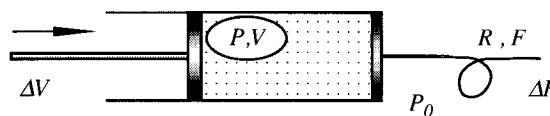


Figure 2. Syringe pump damping system: ΔV , pump fluctuations; P , pressure in the syringe, V , actual bubble volume; P_0 , atmospheric pressure, R , resistance-to-flow of the capillary; F , flow rate; ΔF , flow rate fluctuations.

Procedures. The glassy carbon UniJet working electrode was cleaned daily using a wet, dust-free paper tissue. The time necessary for equilibration at an applied potential of -200 mV vs Ag/AgCl was relatively short (30 min).

Syringes were partially filled by the perfusion solution. Following the removal of all air bubbles, the damping air bubble was drawn into the syringe. Its volume was controlled at $\pm 20\%$ using the calibrated scale of the syringe. This bubble was positioned next to the Teflon piston tip, where it remained throughout the experiment. Finally, the syringe was completely filled, positioned in the microinjection pump, and connected to the flow system via the R-capillary.

RESULTS AND DISCUSSION

Considering the syringe pump damping system depicted in Figure 2, the relationship between pressure and flow rate on the capillary for low flow rates can be described as follows:

$$\Delta P = P - P_0 = RF \quad (1)$$

where F is the flow rate ($\mu\text{L min}^{-1}$), P is the pressure inside the syringe (Bar), P_0 is the atmospheric pressure, and R is the resistance-to-flow of the capillary ($\text{bar}/\mu\text{L min}^{-1}$). The last parameter was estimated using an HPLC pump with a manometric module connected to a capillary, and the pressure under constant flow rate was recalculated. The elasticity of the gas bubble can be expressed by the following ideal gas equation,

$$P_0 V_0 = PV \quad (2)$$

where V_0 is the initial volume of the bubble (μL , at atmospheric pressure), and V is the volume of the bubble under flow rate F and pressure P . The combination of eq 1 and eq 2 gives

$$F = P_0 \frac{V_0 - V}{RV} \quad (3)$$

and the first derivative of eq 3 is

$$\frac{dF}{dV} = -\frac{P_0 V_0}{R} \frac{1}{V^2} \quad (4)$$

By assuming that pump fluctuations are expressed as changes in bubble volume, ΔV , the flow rate fluctuations, ΔF , can be calculated as

$$\int_F^{F+\Delta F} dF = -\frac{P_0 V_0}{R} \int_V^{V+\Delta V} \frac{1}{V^2} dV \quad (5)$$

- (13) Berners, M. O. M.; Boutelle, M. G.; Fillenz, M. *Anal. Chem.* **1994**, *66*, 2017–2021.
- (14) Moscone, D.; Pasini, M.; Mascini, M. *Talanta* **1992**, *39*, 1039–1044.
- (15) Obrenovitch, T. P.; Koshy, A.; Zilkha, E.; Richards, D. A.; Bennetto, H. P. *Curr. Sep.* **1993**, *12*, 48–49.
- (16) Zilkha, E.; Koshy, A.; Obrenovitch, T. P.; Bennetto, H. P.; Symon, L. *Anal. Lett.* **1994**, *27*, 453–473.
- (17) Yang, L.; Kissinger, P. T.; Ohara, T.; Heller, E. *Curr. Sep.* **1995**, *14*, 31–35.
- (18) Coyle, J. T.; Puttfarcken, P. *Science* **1993**, *262*, 689–695.
- (19) Hyslop, P. A.; Zhang, Z.; Pearson, D. V.; Phebus, L. A. *Brain Res.* **1995**, *671*, 181–186.
- (20) Baker, A. J.; Zornow, M. H.; Scheller, M. S.; Yaksh, T. L.; Skilling, S. R.; Smullin, D. H.; Larson, A. A.; Kuczenski, R. *J. Neurochem.* **1991**, *57*, 1370–1379.
- (21) Obrenovitch, T. P.; Richards, D. A. *Cerebrovasc. Brain Metab. Rev.* **1995**, *7*, 1–54.
- (22) Bohs, C. E.; Linhares, M. C.; Kissinger, P. T. *Curr. Sep.* **1994**, *12*, 181–186.

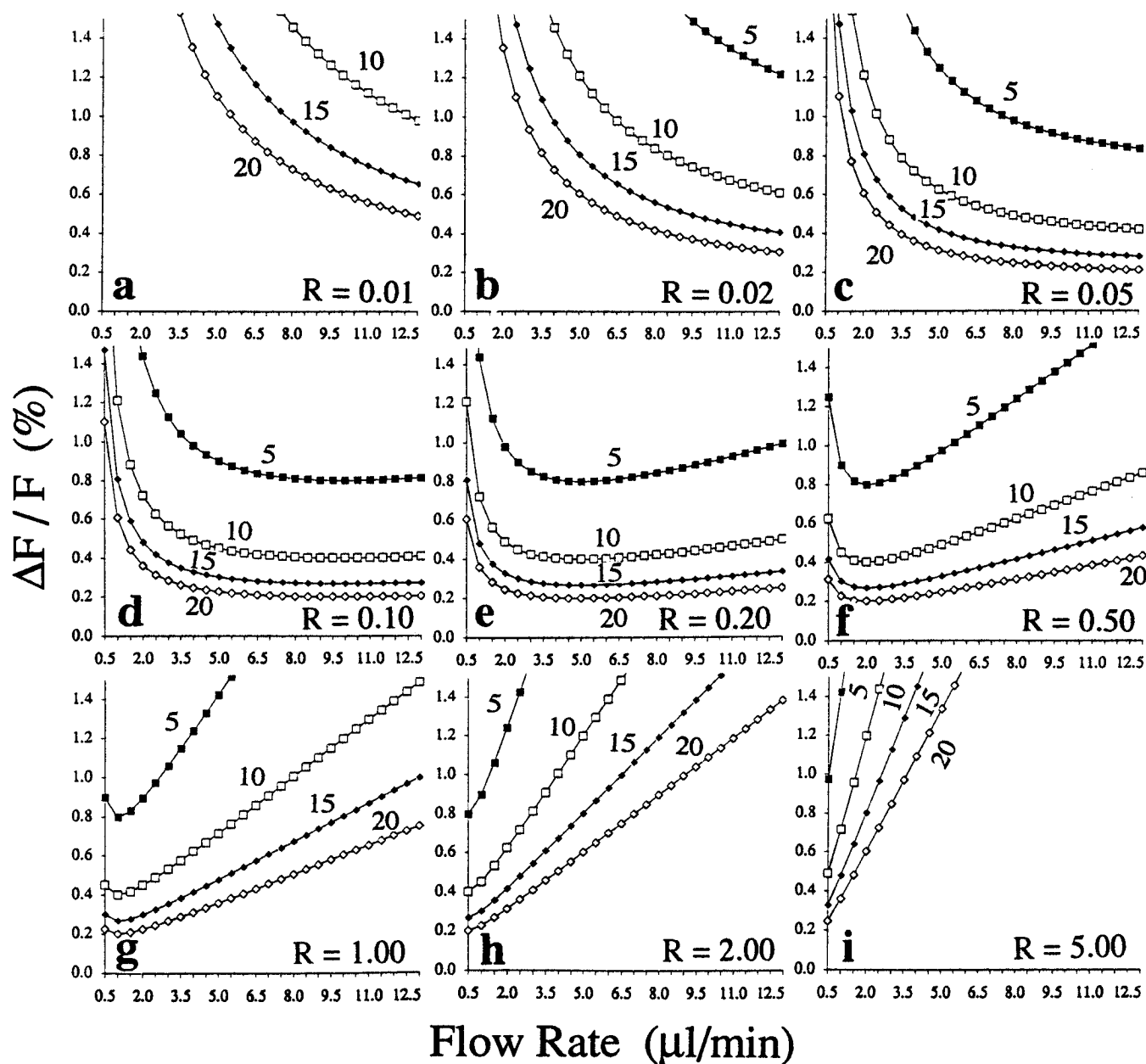


Figure 3. Simulations of different damping systems based on calculations using eq 6 ($\Delta V = 0.01 \mu\text{L}$). R is the constant of the capillary ($\text{bar}/\mu\text{L min}^{-1}$). Each curve is labeled by the value of V_0 (μL).

Solution of eq 5 for $P_0 = 1$ bar gives

$$\left| \frac{\Delta F}{F} \right| = 1 + \frac{1}{RF} - \frac{1}{RF \left(\frac{1}{RF + 1} + \frac{\Delta V}{V_0} \right)} \quad (6)$$

Assuming that the pump fluctuations (expressed as ΔV) are constant in time, the fluctuations of flow rate (ΔF) depend on the bubble volume, V_0 , and the capillary resistance, R , as shown in Figure 3. This figure represents mathematical simulations of eq 6 for different combinations of V_0 and R values. The $\Delta F/F$ ratio is directly related to the noise-to-signal ratio of the system. Ideally, both ratios should be low across all values of flow rate. When the resistance is too low, the $\Delta F/F$ ratio is high at low flow rates (Figure 3a–c). Figure 3d–f depicts the optimum resistance R (minimum of $\Delta F/F$ vs flow rate function) for a $20 \mu\text{L}$ bubble,

which is between 0.1 and $0.5 \text{ bar}/\mu\text{L min}^{-1}$. When the resistance is too high, i.e., $R > 1 \text{ bar}/\mu\text{L min}^{-1}$, the $\Delta F/F$ ratio increases upon raising the flow rate (Figure 3g–i). Under these conditions, the pressure in the system increases.

The effect of high pressure (high flow rate and/or high R) on gas solubility should also be mentioned. Since the bubble consists of a gas (air, nitrogen, etc.), the gas dissolution into the liquid filling the syringe will increase as a function of pressure following Henry's law. Similarly, when the pressure decreases, the gas will be excluded from the solution as small bubbles. This degassing phenomenon will likely occur in the detector, where the pressure is close to the atmospheric pressure, giving rise to unstable EC signals. However, under our conditions ($R = 0.23$, flow rate $< 5 \mu\text{L min}^{-1}$, $\Delta P < 1.15$ bar) this phenomenon is not observed.

The bubble size is also a limiting factor for practical use. The larger is V_0 , the better is the damping effect (i.e., low $\Delta F/F$ ratio), but a longer time will be necessary in order to stabilize the flow

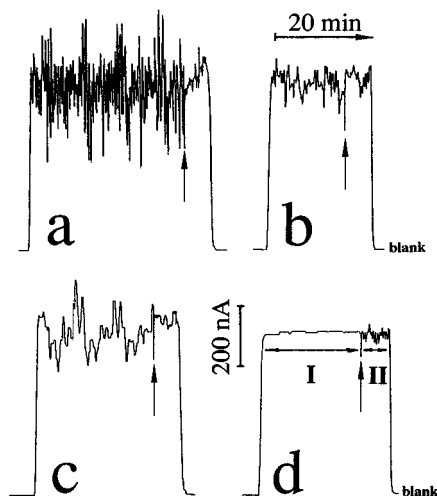


Figure 4. Steady state response of 100 μM 1,4-benzoquinone. Glassy carbon at -200 mV vs Ag/AgCl , pH 3.0, flow rate 2 $\mu\text{L/min}$. (a) Nondamped, (b) 15 cm capillary, (c) 20 μL bubble, (d) 15 cm capillary and 20 μL bubble. The arrow within each quinone signal represents a change between the two pumps.

rate and baseline current. A bubble volume of 20 μL shows a stabilization time of maximum 30 min.

Taking into account all of these factors, the optimum performance with a 20 μL bubble and a 15 cm capillary length ($R = 0.23\text{ bar}/\mu\text{L min}^{-1}$) was achieved by using a flow rate between 1 and 5 $\mu\text{L min}^{-1}$.

The positive effect of a well-damped, in contrast to an undamped, flow system is shown in Figure 4. Figure 4a corresponds to the steady state reduction current of 100 μM quinone at -200 mV vs Ag/AgCl at a glassy carbon electrode using no damper at all. The transition at the start and finish of each set is due to switching blank perfusion buffer versus the same buffer with quinone. In the beginning of the trail, the pulses are not randomly distributed and are due to the stepping of the motor of

the microinjection pump. We observed a similar phenomenon with respect to the distribution of noise peaks when using an HPLC piston pump (results not shown). As expected, the capillary without the bubble (Figure 4b) or with a bubble but without the resistive capillary (Figure 4c) cannot dampen pulsation to the extent observed for the complete damper (i.e., bubble + capillary, Figure 4d). The arrow in Figure 4 represents the switch from one pump to the other. As we may see comparing regions I and II in Figure 4d, pump 2 is less affected by the damping modification than pump 1. Such a different "handwriting" between pumps was also observed between different syringes due to differences in points of friction between piston tips and glassy syringe bodies.

CONCLUSION

A substantial reduction of the background noise generated by the pump system in microdialysis coupled on-line with amperometric detection was successfully achieved by using the combined effects of capillary and an air bubble entrapped in the syringe. This setup, with the new damping system, opens up the possibilities of improved detection for low levels of compounds for in vivo analysis. Enhancements of the limit of detection by 2 orders of magnitude are observed for the analysis of quinones in dialysates from reperfused ischemic rat brain. Successful results at the micromolar level are currently obtained using this experimental setup on freely moving rats and will be published in a near future.

ACKNOWLEDGMENT

The authors are indebted to BAS for instrumental setup. M. P. thanks the Department of Pharmaceutical Chemistry and Drug Analysis, Vrije Universiteit Brussel, for financial support.

Received for review February 28, 1996. Accepted April 26, 1996.[®]

AC9601977

[®] Abstract published in *Advance ACS Abstracts*, June 1, 1996.